

NUMERICAL ANALYSIS OF THE LOW VELOCITY REGIONS IN AN ARRAY OF THREE HORIZONTAL 90° ELBOWS CONDUCTING WATER.

V. Vera Arenas⁽¹⁾, F. Sánchez Silva⁽²⁾, Ye. Pysmennyy⁽³⁾, G. Polupan⁽²⁾ and
J. G. Barbosa Saldaña⁽²⁾

⁽¹⁾Master student, LABINTHAP-SEPI-ESIME-IPN, Tel (5)729-6000 ext. 54754

⁽²⁾LABINTHAP-SEPI-ESIME-IPN-COFAA, Av. IPN s/n, UPALM Edif. 5, 3er. Piso, 07738 México, D.F.

Tel (5)729-6000 ext. 54754, E-mail: fsnchz@yahoo.com.mx

⁽³⁾National Technical University of Ukraine "Kyiv Polytechnic Institute",
Pr. Peremogy 37, PC 252056, Kyiv, Ukraine e-mail: rial@i.kiev.ua

ABSTRACT

The numerical simulation and the results analysis, of the velocity and pressure fields in a three 90° elbows horizontal array are presented in this paper. A turbulent water flow ranging in a [44000, 176000] Reynolds number was used for the simulation with Fluent®.

The velocity profile and the static pressure distribution inside the pipe and the three elbows array were analyzed when the separation distance between the elbows 1 - 2, and 2 - 3 were changed. The pipe diameter used for the simulation was 44 mm, and all the elbows had an average curvature radius of 100 mm. the tested separation between the elbows (L_1 and L_2) was varied from 0D to 10D.

Results show that there is a minimum separation distance between elbows 1 and 2 where there is no more influence on the velocity profile in the first elbow and then the lowest velocity zone could be used for metrology and separation purposes.

Key words: elbows, velocity profile, pressure distribution.

I. INTRODUCTION

It is very surprising to observe the important role that pipelines play in our daily life. For instance the water we use at home and also the waste are transported by means of pipelines. Besides at home, the use of fluids in other economical activities is really enormous, we find it from the process of agriculture products until the manufacture of paper and steel as well. In fact, all the fluids employed in all these processes have to be transported by pipelines. For instance in USA only the oil industry transports more than two millions barrels of oil per day without counting the thousands of millions of cubic feet of gas transported per day using gas pipelines.

In all the pipelines networks for liquids, gases and two-phase mixtures transport, elbows are always present, they are coupling fittings, which are necessary for the pipeline direction changes and to provide mechanical flexibility to the system.

These accessories can be also used as phase separators, in the case of two phase flow transport, where the idea is to take advantage of the centrifugal force which appears in the accessory so that by installing a ramification in the highest pressure zone of the elbow it is possible to extract the liquid phase and then they can work as separators [4, 12]. On the other hand, the radial pressure difference which appears between the internal and external part of the elbow provides a radial pressure difference parameter which can be correlated for its use as flow meters [7, 9].

This work is one of the three stages of the research project where the two-phase separation phenomenon is studied. The main interest is the radial pressure drop distribution and the low velocity regions location occurring when the flow goes through a 90° horizontal elbow. In this first stage a single phase flow going through a combination of three 90° elbows in horizontal position is modeled, the objective is to find the lower and higher velocity regions into the fittings and the pipe itself, which will permit to select the lowest velocity zone and the pipe diameter that must be used as ramification in order to build a phase separator.

In this stage, a single phase water flow is used as the flow going through a combination of three 90° elbows without ramification, the objective is to find out the best geometry where the biggest velocity difference of the flow is obtained, so we can use these results for two phase flow experiments in order to study the phase separation phenomenon.

The numerical simulations were done in 3-D using the κ - ϵ turbulence model provided in the CFD commercial code Fluent®, using elbows with the following characteristics: 44 mm internal diameter, curvature radius 100 mm and the separation between the elbows was varied from 0D to 10 D respectively.

NOMENCLATURE

| | | |
|------|-----------------------|---------|
| A | pipe transversal area | $[m^2]$ |
| D | pipeline diameter | $[mm]$ |
| e | absolute roughness | $[mm]$ |
| L | length | $[m]$ |
| P | pressure | $[Pa]$ |
| Re | Reynolds number | |
| Rc | curvature radius | $[mm]$ |
| t | time | $[min]$ |
| U | velocity | $[m/s]$ |
| X | coordinate | |
| Y | coordinate | |
| Z | coordinate | |

Subscripts

| | |
|------|-------------------|
| 1 | first separation |
| 2 | second separation |
| d | dynamic |
| st | static |
| T | total |

II. METHODOLOGY EMPLOYED

All numerical simulations must be validated using experimental data, because the numerical simulation by itself is not much confident. In the present work experimental data were used to select the most adequate turbulence model and then use it with confidence to determine the mesh independence.

1) *Geometry description and mesh*: In order to select the more adequate turbulence model and to determine the mesh independence, the experimental data obtained by Hernandez [11] using a geometrical array as the one shown in Fig. 1, were employed.

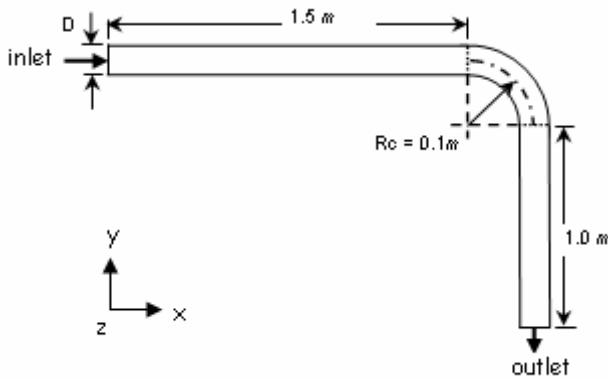


Fig. 1. Geometry characteristics used for the comparison of the experimental data and the turbulence model and the mesh independence study [11].

The mesh of the elbow shown in Fig. 1, is developed in two steps. In the first step the mesh is prepared for the pipe inlet

which is represented schematically in Fig. 2, it has 10 concentric circles with a separation ratio r equal to 0.92 and 20 radial lines ($1D$ length) crossing the symmetry axis equally spaced. As a second step, the mesh was done for all the geometrical body under study, a 20 mm separation was used for all the volumes as shown in Fig. 3. In the elbow this separation was made dividing the curvature radius.

The boundary conditions, for the geometry under study were imposed as follows: 1) a uniform profile velocity was imposed at the pipe inlet equal to 1 m/s , and certain length of pipe was allowed in order to permit the flow to attain its fully developed velocity profile (the velocity profile expected is a turbulent profile which is attained in a distance approximately between $20D$ and $30D$ from the inlet). 2) At the outlet, the mass flow was discharged to the atmosphere, for this reason, the pressure at the exit is taken as zero. 3) Finally in all the remaining surface (pipe walls), is imposed the non-slip condition taking into account that the surface has a relative roughness of $e/D = 0.001$.

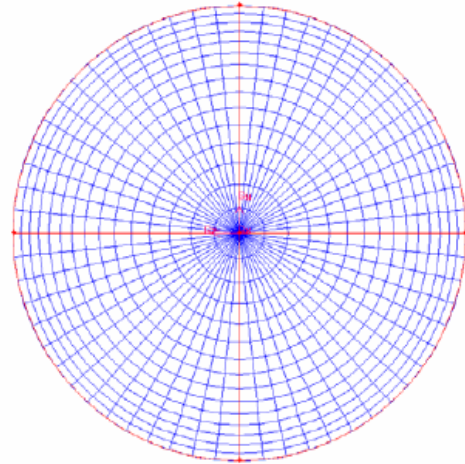


Fig 2. Mesh of the transversal section at the inlet (surface where the flow comes into the pipe).

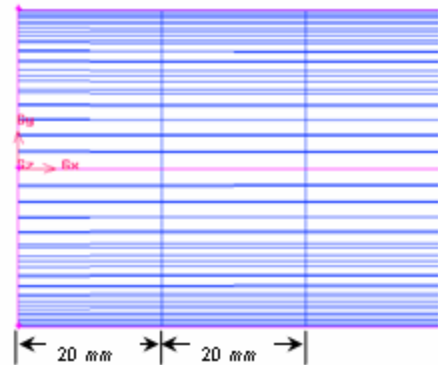


Fig. 3. Separation between the volume elements.

2) *Turbulence model selection*: The turbulence model was selected using the following criterion: 1) That the results of each simulation (using different turbulence models) fit the experimental results; 2) The computation time among the tested models should be the lowest.

For all the simulations a 10x20x2 mesh (ten concentric circles, twenty radial divisions and 20 mm length of the control volume) was used. Static pressure data were taken in the external part of the elbow each 10° respect the inlet of the flow. The time taken for the simulation was also registered for all the tested turbulence models.

For these numerical runs, the following models were tested: κ - ϵ standard, RNG and realizable, and also the models κ - ω normalized and SST. Although in the Fluent® there are included other turbulence models as Spalart-Allmaras, Reynolds Stress and LES (Large Eddy Simulation), these were not used because the first one is used for external flow and the other two models their formulation is much more complete and complex and consume much computational time.

In Fig. 4, the numerical results of the static pressure obtained each 10° are plotted, beginning in the inlet of the elbow, and then they were compared against the experimental results. The two models showing a better approximation are the κ - ϵ standard and the κ - ϵ RNG, but it is important to mention that the κ - ϵ standard model needs less computational time (around one hour and a half less than the κ - ϵ RNG). For this reason, from all five tested models we choose the κ - ϵ normalized.

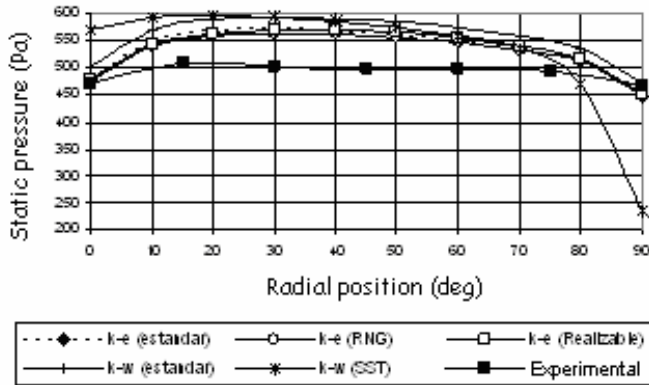


Fig. 4. Comparison of results using different turbulence models and experimental data.

3) *Mesh Independence*: For the mesh independence study the following methodology was used: first, the mesh was refined in the frontal face and finally the separation between the elements of volume was analyzed.

Three kinds of meshes were compared for the frontal face, 10x20x2, 15x30x2 and 20x40x2, where the first number represents the number of concentric circles, the second is the number of lines dividing the circumference and finally the third is the separation between the volume elements.

The mesh independence of the frontal face is attained when the errors in the static pressure of reference are less than 5%. The maximal percent errors for the sensibility comparison are shown in table 1, and the position where it takes place as well.

Table 1. Maximal errors and position where they take place, for the frontal face mesh independence analysis.

| Comparison | Error |
|----------------|--------|
| 10x20 vs 15x30 | 1.417% |
| 15x30 vs 20x40 | 0.048% |

According to the results reported in the table 1, we can infer that the best mesh is the 20x40, but this mesh requires more computational time respect the other two meshes (around 1 hour respect to the mesh 15x30) and then is not viable because when we try to reduce the separation between the volume elements it takes more time for the computational runs. For this reason the 15x30 mesh was conserved because it requires less computational time (compared against the 20x40, around 40 minutes), and its maximal error drops in the permissible range (less than 5%).

In the next step we proceed to change the space between the volume elements, keeping constant the frontal mesh. Four separations between the volume elements were compared 2, 1, 0.5 and 0.25 cm. Table 2 presents the comparison of the percent errors and the position where it happens as well.

Table 2. Maximal errors and position where they take place during the axial mesh independence study.

| Comparison | Error |
|-------------------|--------|
| 2.0 cm vs 1.0 cm | 2.359% |
| 1.0 cm vs 0.5 cm | 6.301% |
| 0.5 cm vs 0.25 cm | 2.998% |

We observe that the percent error does not decrease, on the contrary the error increases, that is because the mesh is not enough refined and it just starts being sensible. So, it is necessary to refine the mesh but the inconvenience is that the computational time increases, around to 14-16 hours (the last mesh) and is not practical to refine more the mesh because this geometry counts only one elbow and in the case of putting two more, the computational time would be increased even more. So we need to use an artifice to make the mesh fine in some places and less refined in others. This artifice reduces the computational time, and will allow us to reduce even more the separation between the volume elements. The description of this idea is shown in Fig. 5.

The notation for distinguishing the mesh is as follows: the two first numbers represent the pipe frontal face mesh (15 circles and 30 radial divisions) and the resting numbers the volume elements separation. For the second case, we have that in the 1.5 m straight pipe there are volume elements uniformly separated 20 mm as far as 300 mm before the elbow, after this point, there is a separation between the volume elements of 2.5

mm which corresponds to the elbow itself and 300 mm after it, and then continuing with a separation of 20 mm. In this way the mesh described is represented as 15x30(2x0.25x2).

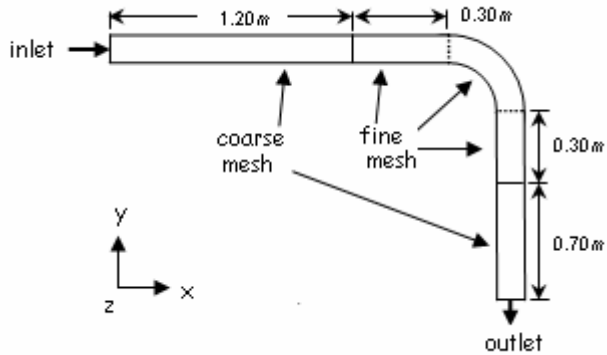


Fig. 5. Mesh refined in some parts of the geometry under study.

In table 3, the maximal errors obtained with the uniform mesh against the non uniform mesh are presented. In the same table we can observe that by refining some parts of the geometry domain it provides good results and the calculation time is reduced in about 1.5 hr.

Table 3. Comparison of the maximal errors in a uniform mesh and non uniform mesh and the point where they are located.

| Comparison | Error |
|---|--------|
| 15x30x0.25 vs 15x30(2x0.25x2) | 0.897% |
| 15x30(2x0.25x2) vs 15x30x(2x0.25x2) only in the elbow | 9.115% |

In table 4 we can observe that the ideal mesh should be the nominated $15 \times 30 \times (2 \times 0.1 \times 2)$, but its computation time is too big (around two more hours than the former). So in order to optimize time and precision in the simulation the $15 \times 30 \times (2 \times 0.125 \times 2)$ was selected, which requires a computation time less than the ideal mesh, although some precision is sacrificed (from an error 0.45% to 2.280 %) we are still in a good confident range (errors lower than 5%).

Table 4. Maximal error for non uniform meshes, with refining only in one part of the geometry (30 cm before and after the elbow and in the elbow itself).

| Comparison | Error |
|---------------------------------------|--------|
| 15x30x(2x0.25x2) vs 15x30x(2x0.125x2) | 2.280% |
| 15x30x(2x0.125x2) vs 15x30x(2x0.1x2) | 0.454% |

For the reasons above mentioned, the optimal mesh, the one using the less computational time and having errors less than 5% is the, $15 \times 30 \times (2 \times 0.125 \times 2)$. This mesh will be used in the three 90° combined elbows study which is the main

objective of this work.

4) *Experimental design*: once the turbulence model is selected and having determined the adequate mesh independence, the next step is to apply them to the cases under study in which we intend to evaluate the influence of the separation between the three elbows in the pressure distribution both in the interior and exterior of the elbows.

The pipeline internal diameter used was 44 mm. The flow enters a 1.5 m length straight pipe, in which the flow will develop and then goes into a zone where three elbows are connected horizontally in a consecutive manner. The elbows are separated by straight pipes of length L_1 and L_2 (these two distances are the variables of the present study) and at the exit of the third elbow it follows a straight pipe of 1.0 m length, used just to avoid exit effects, as shown in figure 6.

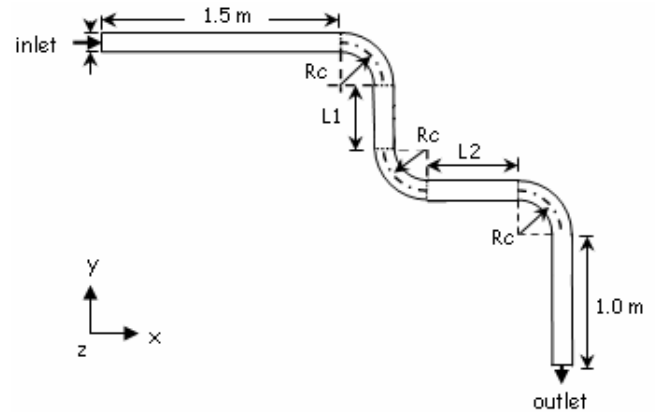


Fig. 6. General representation of the geometry of the cases under study.

The straight pipes L_1 and L_2 are varied from 0D to 10D, with increments on L_1 equal to 2D and 5D for L_2 . With the above mentioned information, a test matrix is obtained, (table 5). In this table we can observe that there are 18 cases of study, in which we pretend to see the elbows separation effect on the pressure distribution on the wall pipes and the flow velocity profile as well.

Tabla 5. Test matrix for the cases under study.

| | | L2 | | |
|----|-----|----|----|-----|
| | | 0D | 5D | 10D |
| L1 | 0D | 1 | 7 | 13 |
| | 2D | 2 | 8 | 14 |
| | 4D | 3 | 9 | 15 |
| | 6D | 4 | 10 | 16 |
| | 8D | 5 | 11 | 17 |
| | 10D | 6 | 12 | 18 |

III. RESULTS AND DISCUSSION.

As it is well known, the velocity profile distorts when passes through any obstacle inside a pipe, but not only the

speed suffers a change, but the static pressure on the pipe wall, since the static and dynamic pressures P_{st} and P_d are very close related with the total pressure P_T . In all the cases it was observed that the static pressure suffers a great distortion when the flow goes through the elbows, producing important variations of pressure along the fitting, creating low and high velocities in opposite sense of the static pressure P_{st} reduction.

The total pressure P_{st} along the pipe was monitored in two sides (figure 7), the external part identified with the upper line of the pipe and the internal line identified with the inferior line.

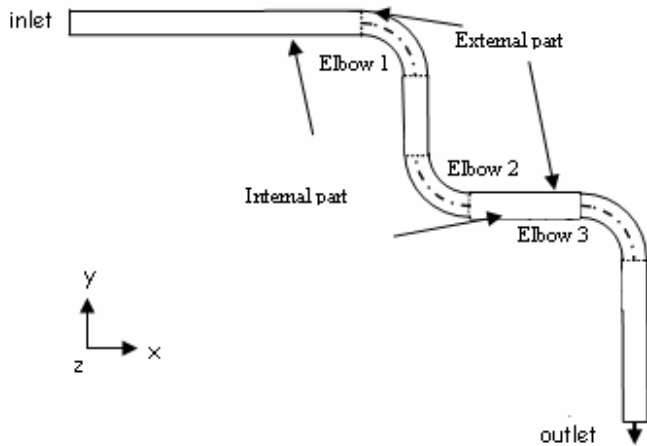


Fig. 7. Schematic representation of the line where the static pressure was monitored.

The analysis starts with the case 1, which is the critical one, where L_1 and L_2 are zero (table 1). The static pressure P_{st} along the pipe is plotted in Fig. 8 and the details of the static pressure in the elbows zone are shown in Fig. 9. In Fig. 8 we observe that the static pressure is the same for both the internal and the external parts of the straight pipeline, but they are different in the elbows zone where the P_{st} of the external part has an increment that prevails up to the region of 30-50°, and after this zone the static pressure reduces. On the other hand the P_{st} of the internal part diminishes up to the region of 30-40° and after this region the pressure increases again. This same phenomenon appears in the other two elbows. Out of the elbows zone there is a region where the P_{st} of both internal and external parts have the tendency to become equal and they attain this condition in a region between 5D to 10D downstream the third elbow.

In Fig. 10, the effect of the three elbows presence on the velocity profile distortion is presented (case 1). In the same figure, it is possible to visualize the low and high velocity regions. The results show that the velocity distribution is opposite to the static pressure distribution, that is in the zone of low velocity there is the region of high pressure and vice versa, in accordance with the energy conservation law. Near the external part, the velocity decreases considerably until the range 30-40°, and up to this region it starts again to increase and tries to recover the velocity it had before coming into the elbow. For the internal part of the first elbow it happens that the

velocity increases due to the low pressure in this zone and then it tends to decrease.

The second elbow effect is to reduce even more the velocity coming from the first elbow producing, in this way, a region of lower velocity (when compared with an array of one elbow). This circumstance is beneficial for the phase separation case where, the difference of pressure induces the higher density phase goes to the low velocity region. With this result we can say that the two elbows combination produce a velocity reduction in certain regions where we can install a branch pipe for the phase separation purposes.

The presence of the third elbow produces only a small additional velocity reduction, as it is shown in figure 10, there is only a small pipe section where the velocity reduces. We can say that a third elbow does not produce additional reduction of the velocity in any region, and that it is enough to have two elbows to produce the effect we are looking for.

The separation length between the elbows plays a very important role, because when L_1 is bigger than $6D$, the effect of the first elbow on the second elbow velocity field (velocity reduction in the second) almost disappear, and then the second elbow behaves like the first and the third like the second since the point of view of flow behavior, repeating the same phenomenon in shape and magnitude, keeping L_2 equal to $0D$.

IV. CONCLUSION

The numerical simulation is a useful tool for the solution of engineering problems overall the kind of problems where it is expensive and complicated to run experiments.

The static pressure perturbation P_{st} in the internal and external part of the pipeline begins approximately 1D before the first elbow and continues up to 10D downwards the third one. The maximal and minimal P_{st} from the internal and external sides of the elbow takes place in the interval of 30 to 50°.

The velocity profile is affected in the same way as the P_{st} is, starting 1D upwards the first elbow, except that the velocity profile does not develop completely in a distance of 25D downwards. It is possible to reduce even more the flow velocity in certain parts of the pipe by means of the combination of two elbows as minimum; the reduction can be even one third of the average velocity inside the pipe ($V_{prom} = 1.0 \text{ m/s}$) and this low velocity region covers almost a quarter of the pipe section this takes place in the second elbow.

If the separation between the first and the second elbow L_1 exceeds $6D$, and L_2 is kept constant and equal to $0D$, the velocity profile of elbows 2 and 3 have much similitude with the results of the elbows 1 and 2 (case 1).

ACKNOWLEDGMENTS

The authors thank the Researchers Formation Program of the National Polytechnic Institute of Mexico for the economical support to the students and COFAA and EDI program for the economical support to professors.

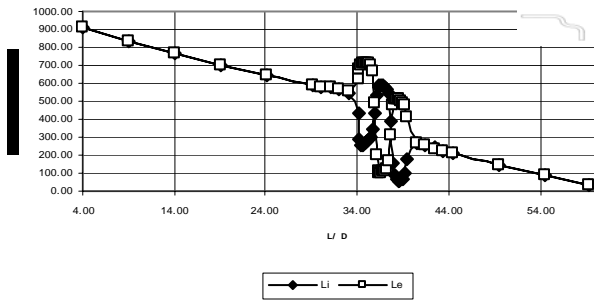


Figure 8. Static pressure distribution along the pipe (internal and external walls) case 1.

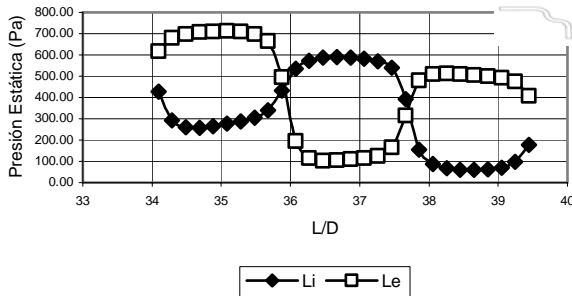


Figure 9. Static pressure distribution in the elbows zone (internal and external walls) case 1.

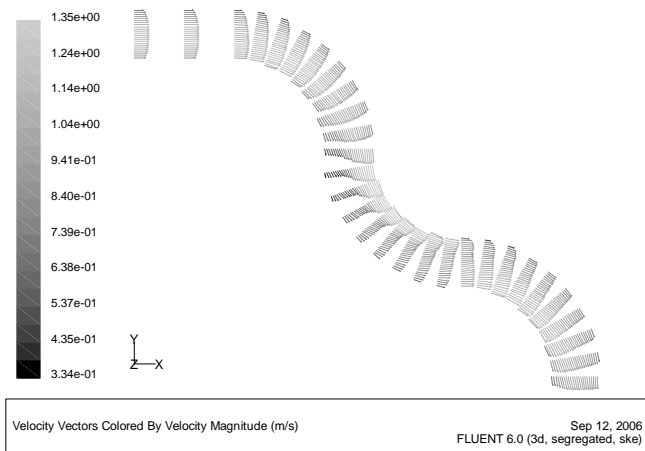


Figure 10. Velocity profile in the elbows section, case 1.

REFERENCES

- [1] **F. Elizalde B.** et al, “Obtención experimental y validación numérica mediante CFD de pérdidas de presión en accesorios”, 4° CHIES, Cd. México DF., 18-21 de Noviembre de 2005.
- [2] **F. Sánchez S.** et al, “Experimental Characterization of Air-

Water Slug Flow Through a 90° Horizontal Elbow”, Two-Phase Modelling and Experimentation 1999, pp. 827-834.

[3] **A. Mukhtar, et al**, “Pressure Drop in a Long Radius 90° “Horizontal Bend for the Flow of Multisized Heterogeneous Slurries”, Int. J. Multiphase Flow, Vol. 21 No.2 pp. 329-334. 1995.

[4] **V. Hernández P., et al**, “Study of the 90° Elbows Performance as Phase Separators in an Air-Water Two-Phase Flow”, 4th ASME JSME Joint Fluids Engineering Conference, Honolulu, Hawaii, USA, July 6-10, 2003.

[5] **R. D. Coffield, et al**, “Irrecoverable Pressure Loss Coefficients for Two Elbows”, ASME Fluids Engineering Division Summer Meeting, June 22-26, 1997.

[6] **Gerald L. Morrison**, “Flow Field Development Downstream of Two in Plane Elbows”, ASME Fluids Engineering Division Summer Meeting, June 22-26, 1997.

[7] **F. Sánchez S., et al** “Experimental Study for the Use of Elbows as Flowmeters”, ASME Fluids Engineering Division Summer Meeting, June 22-26, 1997.

[8] **H. E. Fiedler**, “A Note on Secondary Flow in Bends and Bend Combinations”, Experiments in Fluids 23(1997), pp. 262-264.

[9] **F. Sánchez S., et al**, “Curved Pipe Flow Numerical Simulations for Metrology Purposes Using CFD 2000”, ASME Fluids Engineering Division Summer Meeting, June 21-26, 1998.

[10] **J. W. Murdock, et al**, “Performance Characteristics of Elbow Flowmeters”, Transactions of the ASME, September 1964, pp. 498-506.

[11] **Justo Hernández Ruiz**. “Estudio del Comportamiento del Campo de Flujo en Tuberías Curvas para su Aplicación en Metrología”. Sección de Estudios de Posgrado e Investigación ESIME-IPN México D. F. 27 de marzo de 1998.

[12] **Azzopardi B. J. et al**. “Plant application of a T junction as a partial phase separator”, Trans. I. Chem. E80 A, pp. 87-96 (2002).